BOLETIM

Sociedade Portuguesa de Hemorreologia e Microcirculação

Bulletin of the Portuguese Society of Hemorheology and Microcirculation

Vol. 25 n.º 2 Abril, Maio, Junho 2010

Sumário / Summary

Sociedade Portuguesa de Hemorreologia e Microcirculação

Presidente Honorário: Prof. Doutor João Alcindo Martins e Silva

ÓRGÃOS SOCIAIS DA SPHM / BOARDS (2007-2009)

Direcção / Executive Committee

Presidente
Prof.ª Doutora Maria Carlota
  Saldanha Lopes

Vice-Presidentes
Prof. Doutor J. M. Braz Nogueira
Prof. Doutor Carlos Perdigão

Secretário-Geral
Dr. José António Pereira Albino

Tesoureiro
Prof. Doutor Flávio Reis

Secretários-Adjuntos
Prof. Doutor Henrique Luz Rodrigues
Prof. Doutor J. Ducla Soares
Dr. Jorge Lima

Assembleia Geral / General Assembly

Presidente
Prof. Doutor A. Diniz da Gama

1.º Secretário
Dr. João Paulo Guimarães

2.º Secretário
Dr. Miguel Frederico Leal Galvão

1.º Secretário Suplente
Dr. Luís Sargento

2.º Secretário Suplente
Dr. Paulo Ferreira da Silva

Conselho Fiscal / Finance and Audit Committee

Presidente
Prof. Doutor Victor Oliveira

1.º Vogal
Dr.ª Maria Helena Baptista Manso Ribeiro

2.º Vogal
Dr. Carlos Manuel dos Santos Moreira

Comissão de Delegados / Committee of Delegates

Delegado da Região Norte
– Dr. Manuel Campos
Delegado da Região Centro
– Dr. João Morais
Delegado da Região Sul e Regiões Autónomas
– Dr. Mário Marques

MEMBROS CONSULTIVOS, HONORÁRIOS E CORRESPONDENTES / / CONSULTIVE, HONORARY AND CORRESPONDENT MEMBERSHIP

Conselho Científico / / Scientific Council

A. Diniz da Gama
Axel Pries
Fernando Lacerda Nobre
Helena Saldanha Oliveira
J. Esperança Pina
J. Luís Providência
J. Martins e Silva
J. Fernandes e Fernandes
J. Rafael Ferreira
João Morais
José Ferro
Manuel Carrageta
Mário Andreia
Ricardo Seabra Gomes

Sócios Honorários / / Honorary Members

A. M. Ehrly (Alemanha)
Carlos Ribeiro (Portugal)
H. J. Meiselman (EUA)
Helmut Drexler (Alemanha)
J. F. Stoltz (França)
J. E. Tooke (G. Bretanha)
John A. Dormandy (G. Bretanha)
Joaquim Silva Carvalho (Portugal)
J. M. G. Toscano Rico (Portugal)
L. Teixeira Diniz (Portugal)
M. Boisseau (França)
Políbio Serra e Silva (Portugal)
Sandro Forconi (Itália)
Y. Isogai (Japão)

Sócios Correspondentes / / Correspondent Member

Adrian J. Barnes (G. Bretanha)
Alon Harris (USA)
D. Seiffge (Alemanha)
G. Caimi (Itália)
G. D. O. Lowe (G. Bretanha)
I. Juhan-Vague (França)
I. Salama Benarroch (Argentina)
J. Delaunay (França)
J. F. Brun (França)
Ricardo Manrique (Brasil)
Shi Yong-de (China)
T. Shiga (Japão)
Thao Chan (França)

FILIAÇÃO INTERNACIONAL
EUROPEAN SOCIETY FOR CLINICAL HEMORHEOLOGY
EUROPEAN SOCIETY FOR MICROCIRCULATION

SINALIZAÇÃO NO ERITRÓCITO/ERYTHROCYTE SIGNALLING

O eritrócito tem merecido destaque em notas de abertura deste boletim e tem sido objecto de mais de oito mil artigos de revisão referenciados na página do *Pubmed*.

Além das suas funções de transporte de gases (como o oxigénio, o monóxido de carbono e o anidrido carbónico), hemorreológicas, imunológicas e anti e pró – oxidantes, exerce ainda funções de sinalização a longa distância. A associação entre as capacidades funcionais e os estados inflamatórios de curta ou longa duração é relatada em publicações de muitas revistas de elevado índice de impacto. Questiona-se a este respeito se a inflamação (os seus marcadores) e a agregação eritrocitária são precursores ou repercussões do enfarte do miocárdio agudo. O trabalho do grupo de israelita de Arie Steinvil publicado em *Clinical Research Cardiology* , de Maio deste ano, indica que são consequências.

O avanço da tecnologia (p. ex., a microscopia holográfica digital) aplicada ao eritrocito tem possibilitado a quantificação de modo não invasivo, sem recorrer a artefactos nem a marcadores fluorescentes, p. ex., os índices volumétricos e o teor em hemoglobina eritrocitária. A relevância funcional do eritrocito, acrescida à de marcador de prognóstico e de diagnóstico e à utilização como modelo experimental, faz dele um relevante objecto de investigação científica, em

que se inclui o aumento do conhecimento sobre as suas propriedades como resultado da aplicação de metodologias de tecnologicamente sofisticadas.

Ainda não se entendem completamente as causas que trazem tantos insucessos às transfusões sanguíneas, nomeadamente dificuldades hemorreológicas e distúrbios hemostáticos e vasculares, onde o eritrocito é parceiro e mediador de interacção celulares. Estamos a falar de um corpúsculo sanguíneo sem núcleo, com 120 dias de tempo de vida média em condições normais mas que diminui, por vezes substancialmente, em estados de hemoglobinopatia ou membranopatia, entre outras patologias. A multiplicidade de eritrocitos com idades diferentes que compõem o fluxo sanguíneo naquelas situações explica a enormidade de estudos realizados sobre os mecanismos de eriptose (apoptose celular), de senescência, de remoção fagocitária e de interacção com a célula endotelial. Relativamente a esta última muito tem sido descrito sobre a adesão ao endotélio vascular dos drepanocitos e dos eritrocitos, quer infectados pelo parasita plasmódio *falciparum* (neste caso a adesão é mediada por moléculas do parasita) quer provenientes dos doentes com diabetes tipo II.

Trabalhos desta década revelaram que a membrana eritrocitária possui CD44 com capacidade de interactuar

com o ácido hialurónico da célula endotelial,embora na dependência da idade globular. Assim, eritrocitos mais velhos e, consequentemente com menos ácido siálico, interactuam e rolam em condições de baixa tensão de cisalhamento. Este pode ser um processo explicativo da captura dos eritrocitos da circulação sanguínea pelo sistema retículo endotelial do baço. Ainda que a remoção CD44- dependente não seja influenciada de modo directo pelo estado inflamatório, um estudo recente (publicado no www.jbiomedsci. com), realizado *in vitro* revelou que a concentração de ácido hialurónico está aumentada em circulação naquela situação. A interacção do ácido hialurónico com o glóbulo vermelho induz aumento da rigidez, diminuição da deformabilidade e da agregação eritrocitárias.

Muito, há ainda a percorrer para juntar todas as peças, do *puzzle*, já que cada uma delas é fascinante potencialmente geradora de muitas mais.

Que esta breve nota vos suscite curiosidade, é o meu desejo.

Carlota Saldanha
Presidente da SPHM

TOMOGRAFIA QUANTITATIVA DE FLUORESCÊNCIA DAS ALTERAÇÕES VASCULARES DA PROGRESSÃO TUMORAL E TRATAMENTO *IN VIVO* / QUANTITATIVE FLUORESCENCE TOMOGRAPHY OF VASCULAR CHANGES IN TUMOR PROGRESSION AND TREATMENT IN VIVO

*Jeffrey D. Peterson**

ABSTRACT

Recent advances in photonic technology have taken optical imaging beyond standard, qualitative two-dimensional fluorescence reflectance imaging into the realm of three-dimensional fluorescence molecular tomography (FMT™) for non-invasive imaging of deep tissue localization and quantification of fluorescence in living animals. High quality images and accurate quantification of fluorescent agents in deep tissue *in vivo* is achieved by imaging within the near-infrared spectral region (600-900 nm), which minimizes tissue light absorption and allows the transillumination (*i.e.* the passing of light completely through the body) of experimental subjects. The pairing of powerful, deep tissue FMT imaging (VisEn Medical) with the injection of appropriate near infrared (NIR) fluorescent imaging agents allows the detection and quantification of important biological processes and disease pathways in a variety of mouse models of disease conditions without the need for genetically modified cells or animals. Using this imaging approach, quantitative fluorescent measurements can be made to assess cellular protease activity in cancer, inflammation, and stroke (ProSense™, Cat B FAST™, MMPSense™), changes in bone turnover in arthritis, osteoporosis, and bone fracture (OsteoSense™, Cat K FAST™), the induction of apoptosis (Annexin-Vivo™), and many other disease states.

Changes in vascularity and vascular function in oncology and inflammation can also be imaged with a variety of fluorescent agents, including IntegriSense™, which detects $\alpha_v\beta_3$ integrin expression associated with neovascularization, and a variety of vascular agents (AngioSense™, Superhance™, AngioSPARK™) that differ in their size, biodistribution, and pharmacokinetic properties. The integrin $\alpha_v\beta_3$ is significantly upregulated in tumor cells and activated endothelial cells during angiogenesis, but it is not increased in quiescent endothelium. This imaging agent has been used both as a mechanistic biomarker for integrin antagonist therapy and to image anti-angiogenic therapeutic efficacy in mouse oncology studies. AngioSense™ has been

* VisEn Medical Inc., Medford, Massachusetts, USA.

A. FMT 2500 Imaging

B. FMT 2500 Quantification
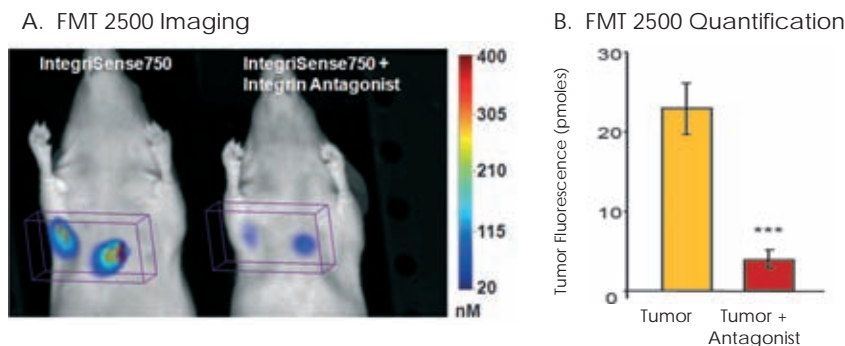
Figure 1 – Imaging selective $\alpha v \beta 3$ **targeting with IntegriSense 750.** Normal Nu/Nu mice (n = 5 mice per group) were injected subcutaneously in both upper mammary fat pads with 4T-1 mouse breast adenocarcinoma cells. Tumors were allowed to grow for 7 days, at which time mice were injected intravenously with 2 nmoles of IntegriSense750, with or without co-injection of excess (100 nmoles) integrin antagonist. **(A)** Mice were imaged by FMT 2500 24h after IntegriSense750 injection and are represented as 3 dimensional images with tumor regions selected by a 3D region of interest (ROI). **(B)** Fluorescence tomographic datasets were analyzed to determine the total amount of fluorescence (in pmoles) in each tumor. Significant decreases in total tumor fluorescence were seen in mice receiving the integrin antagonist supporting the *in vivo* selectivity of integrin imaging. Data are representative of three separate experiments. Asterisks represent changes with statistical significance, *** $p<0.001$

used to non-invasively, and in real-time, detect tumors and quantify the very early vascular changes associated with anti-angiogenic therapy. AngioSense localizes to the vasculature 1 hr after injection and extravasates into the surrounding tissue by 24 h, identifying regions of increased vascular leak. In anti-angiogenic treatment studies, we have found that standard tumor size measurements (by calipers) detect marginally significant tumor changes by day 7 post-treatment, whereas FMT imaging at 24 h quantified the dramatic biological changes in vascular leak that preceded tumor regression by several days. These studies illustrate the potential of NIR fluorescence imaging to non-invasively quantify the underlying biology of vascular processes in real time, crucial in the development and monitoring of anti-angiogenic therapies.

A.

B.
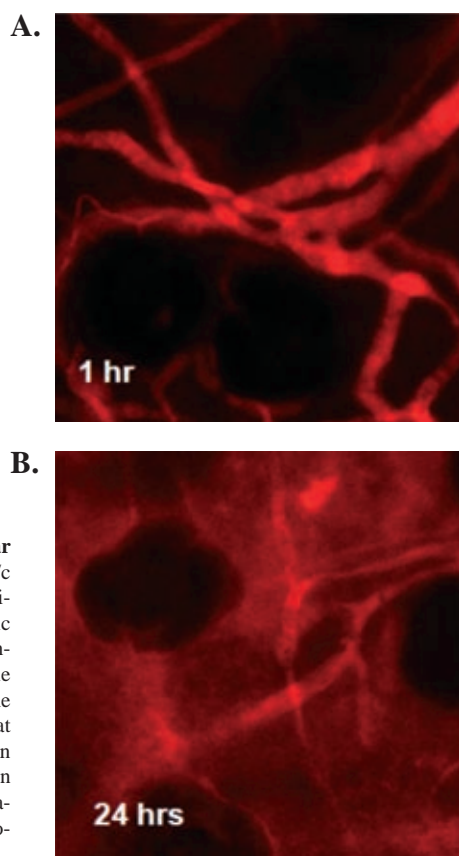
Figure 2 – Imaging vascularity and vascular leak with AngioSense 680. Normal BALB/c mice were injected i.v. with 2 nmoles of AngioSense 680. Noninvasive confocal microscopic imaging of blood vessels in the ear shows AngioSense680 localization exclusively in the vasculature at 1 hr, with extravasation into the surrounding tissue apparent at 24 hr. Imaging at 24h with AngioSense680 allows the detection of functional vascular leak changes, with even greater rates of leakage (and agent accumulation) know to occur in sites of edema or angiogenesis
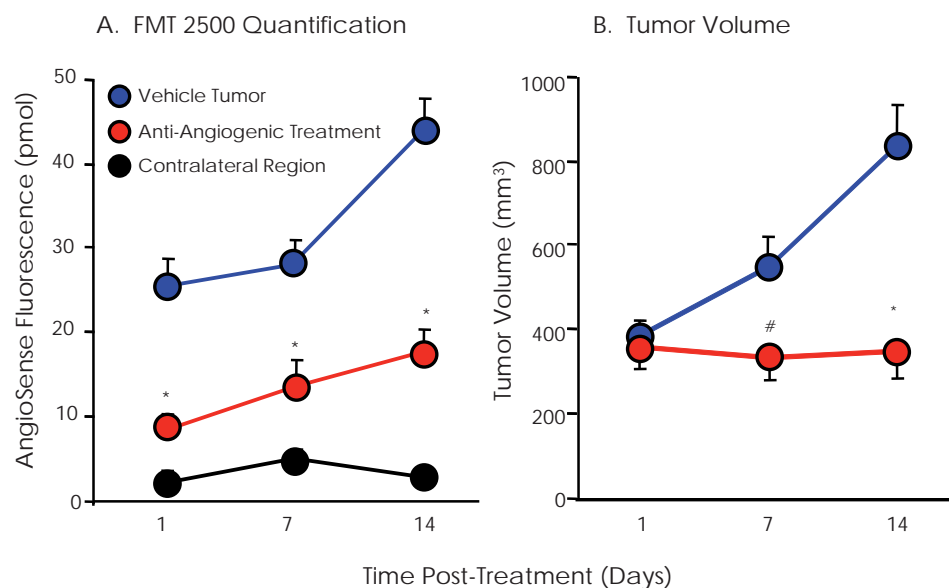
Figure 3 – Early detection of anti-angiogenic efficacy by AngioSense imaging of 24h vascular leak. BALB/c *nu/nu* mice (n = 12 mice per group) were injected subcutaneously in the flank with human colon carcinoma Colo-205 cells. Twelve days later, tumor volumes were measured by caliper, and mice were randomized into 2 groups of equivalent average starting tumor volumes calculated using the formula volume (mm^3) = (length x width^2)/2. Mice were then treated with a targeted anti-angiogenic agent or vehicle. Treatment began on Day 0 and continued three times per week until Day 21. Mice were injected intravenously with AngioSense 680 on Days 0 (3h following first drug treatment), 6, and 13, and imaged 24 hrs later on an FMT Imaging System. **(A)** Fluorescence tomographic datasets from tumor-bearing treated and untreated mice were analyzed to determine the total amount of fluorescence (in pmoles) in each tumor. Significant differences in total tumor fluorescence between animals treated with the anti-angiogenic agent and those animals that received vehicle were revealed within 24 hours of the first treatment (Day 1) and continued to Day 14. The background fluorescence (i.e. the fluorescence quantified in a comparable region of interest on the contralateral flank) showed no observable differences over time. **(B)** No effect on tumor size could be shown using standard caliper assessment at 24h, but by Day 7, tumor size differences were apparent of marginal statistical significance. Data are representative of three separate experiments with different types of anti-angiogenic agents. Asterisks represent changes with statistical significance, # $p<0.05$, * $p< 0.005$

REFERENCES

Matrix Metalloproteinases Contribute Distinct Roles in Neuroendocrine Prostate Carcinogenesis, Metastasis, and Angiogenesis Progression, Laurie E. Littlepage1, Mark D. Sternlicht1, Nathalie Rougier1, Joanna Phillips1, Eugenio Gallo1, Ying Yu1, Kurt Williams2, Audrey Brenot1, Jeffrey I. Gordon3, and Zena Werb1, 1Department of Anatomy, University of California, San Francisco, California; 2VisEn Medical, Inc., Bedford, Massachusetts; and 3Center for Genome Sciences, Washington University School of Medicine, Saint Louis, Missouri, Cancer Res; 70(6) March 15, 2010.

Dual *In Vivo* Quantification of Integrin-targeted and Protease-activated Agents in Cancer Using Fluorescence Molecular Tomography (FMT) Sylvie Kossodo,1 Maureen Pickarski,2 Shu-An Lin,2 Alexa Gleason,2 Renee Gaspar,2 Chiara Buono,1 Guojie Ho,1 Agnieszka Blusztajn,1 Garry Cuneo,1 Jun Zhang,1 Jayme Jensen,1 Richard Hargreaves,2 Paul Coleman,2 George Hartman,2 Milind

Rajopadhye,1 Le Thi Duong,2 Cyrille Sur,2 Wael Yared,1 Jeffrey Peterson,1 Bohumil Bednar2, 1VisEn Medical, Bedford, MA(USA, 2Merck Research Laboratories, West Point, PA(USA, Mol Imaging Biol, December (2009).

Near-infrared fluorescence: application to *in vivo* molecular imaging, Scott A Hilderbrand and Ralph Weissleder, Center for Systems Biology, Massachusetts General Hospital/Harvard Medical School, Simches Research Center, Boston, MA , Current Opinion in Chemical Biology, 2009; 14:1-9.

Non-invasive Quantitative Tomography of the Therapeutic Response to Dexamethasone in Ovalbumin-Induced Murine Asthma, Houari Korideck and Jeffrey D. Peterson., VisEn Medical Inc., Bedford, MA, *JPET Fast Forward*. Published on March 17, 2009 as OI:10.1124/jpet.108.147579

Behavior of Endogenous Tumor-Associated Macrophages Assessed In Vivo Using a Functionalized Nanoparticle, 1,2Antoine Leimgruber*, 3, Cedric Ber-

ger*,3, Virna Cortez-Retamozo*, Martin Etzrodt*, Andita P. Newton*, Peter Waterman*, Jose Luiz Figueiredo*, Rainer H. Kohler*,
Natalie Elpek†, Thorsten R. Mempel*,†, Filip K. Swirski*, Matthias Nahrendorf*, Ralph Weissleder*,‡ and Mikael J. Pittet*, *Center for Systems Biology, Massachusetts General Hospital, Harvard Medical School, Boston, MA, USA; †Center for Immunology and Inflammatory Diseases, Massachusetts General Hospital, Harvard Medical School, Boston, MA, USA; ‡Department of Systems Biology, Harvard Medical School, Boston, MA, USA, *Neoplasia* (2009); 11:459-468.

A Near-Infrared Cell Tracker Reagent for Multiscopic In Vivo Imaging and Quantification of Leukocyte Immune Responses. Swirski FK, Berger CR, Figueiredo JL, Mempel TR, von Andrian UH, Pittet MJ, Weissleder R., PLoS ONE. 2007; 2(10): e1075.

Fluorescence Molecular tomography enables in vivo visualization and quantification of nonunion fracture repair induced by genetically engineered mesenchymal stem cells, Zilberman Y, Kallai I, Gafni Y, Pelled G, Kossodo S, Yared W, Gazit D., J Orthop Res (in press), 2007.

CARACTERIZAÇÃO HEMORREOLÓGICA, BIOQUÍMICA E CARDIOVASCULAR NUM MODELO DE DOENÇA RENAL CRÓNICA MODERADA EM RATO / HEMORHEOLOGICAL, BIOCHEMICAL AND CARDIOVASCULAR CHARACTERIZATION OF A RAT MODEL OF MODERATE CHRONIC KIDNEY DISEASE

Garrido P[1], Costa E[2,3], Teixeira-Lemos E\, Parada B[1,4], Teixeira M[1], Santos P[5], Piloto N[1], Sereno J[1], Alves R[6], Pinto R[7], Rocha-Pereira P[3,8], Figueiredo A[4], Nunes S[1], Romão AM[1], Carvalho L[9], Couceiro P[9], Belo L[3,10], Santos-Silva A[3,10], Teixeira F[1,3], Reis F[1,3]

ABSTRACT

Chronic kidney disease (CKD) is a major public health problem throughout the world. The major outcomes include a rapid progression, with development of anaemia and serious complications, namely thromboembolic and cardiovascular events. The pathophysiological alterations depend on the CKD degree, which will also determine the moment to initiate hemodialysis and recombinant erythropoietin (rhEPO) thera-

pies. Thus, the cardio-renal complication might be better prevented or delayed if CKD patients are earlier identified and treated for the associated anaemia, which will depend on a better characterization of moderate stages of CKD. This study aimed to characterization an animal of model of moderate CKD induced by partial (¾) nephrectomy, by evaluating hemorheological, biochemical and cardiovascular profiles. Blood samples from control and CKD rats were collected at 0, 3, 9 and 15 weeks in

[1] Institute of Pharmacology & Experimental Therapeutics, IBILI, Medicine Faculty, Coimbra University
[2] Institute of Health Sciences of University Catholic, Porto
[3] Institute for Molecular and Cellular Biology, Porto University
[4] Service of Urology and Renal Transplantation
[5] Service of Nephrology, Coimbra University Hospital
[6] Functional Genomics Laboratory, Center of Histocompatibility of the Centre, Coimbra
[7] Pharmacology and Pharmacotoxicology Unit, Pharmacy Faculty, Lisbon University
[8] Research Centre for Health Sciences, Beira Interior University, Covilhã
[9] Institute of Anatomic Pathology, Medicine Faculty, Coimbra University
[10] Biochemistry Department, Pharmacy Faculty, Porto University; Portugal.

Corresponding author:
Flávio Reis, PhD
Institute of Pharmacology and Experimental Therapeutics, Medicine Faculty
Sub-Unit 1 (Pólo III), Coimbra University
3000-354 Coimbra, Portugal
Tel: +351239480068; Fax: +351239480073;
E-mail: freis@fmed.uc.pt

order to evaluate: renal function, hemorheological parameters, iron metabolism, blood lipids, peripheral sympathetic and serotonergic systems, redox state and inflammatory markers. BP, tissues trophism indexes and kidney histomorphology were also assessed. Our data is consistent with a sustained moderate degree of CKD with a quickly compensated modest anaemia, though presenting iron metabolism disturbances. Despite the reasonable degree of functionality of the remnant kidney, as suggested by the anaemia correction and by the kidney hypertrophy, several important cardiovascular modifications were developed. Our model presented hypertension, dyslipidaemia, erythropoietic disturbances, sympathetic activation and oxidative stress. This model might be a good tool to study the cellular/molecular mechanisms underlying moderate stages of CKD and to evaluate the therapeutics efficacy for prevention, treatment/correction of cardio-renal anaemia syndromes and complications in early stages.

Key-words: Moderate chronic kidney disease**,** partial nephrectomy, rat model, hemorheological data, renal function, iron metabolism, Cardiovascular profile

INTRODUCTION

Chronic kidney disease (CKD) has been associated with a large number of alterations, namely anaemia, hypertension, inflammation, iron metabolism disturbance, white blood cell activation, oxidative stress and sympathetic overactivation[1-6]. However, the pathophysiological alterations depend on the CKD degree, which will also determine the moment to initiate hemodialysis and recombinant erythropoietin (rhEPO) therapies, for correction of anaemia, as well as its success. Therefore, cardiovascular events, renal failure, and premature death can be prevented or delayed if earlier identified and treated for CKD[6].

Animal models of CKD, achieved by a reduction in nephron number, create the possibility of testing *in vivo* the mechanisms associated to renal dysfunction, and might be essential to study the complications associated to CKD as well as the efficacy of therapeutics to prevent or delay adverse effects. The most common used techniques include surgical resection of the tissue (partial nephrectomy) and infarction[7], but there is yet limited information about its complete characterization, namely for moderate CKD stages, which will restrict the research on the molecular/cellular mechanism underlying the cardio-renal-anaemia syndrome, as well as its therapeutics. There is some evidence that the infarction model in rats presents a significant increase in proteinuria, hypertension and glomerulosclerosis when compared with the model of simple tissue excision (with equivalent reduction of renal mass)[8]. This suggests that partial nephrectomy can provide a better model of CKD in rat[7]. Furthermore, there is some evidence of a good inter-individual variability of uremia in this model of CKD. However, it is difficult to standardize it, due to the lack of consistency of nephron mass reduction, and, thus, to reach the desired degree of uremia. Without a consistent characterization

of the animal models of moderate CKD, and of a further comparison with the human pathophysiology of moderate CKD, the research on the molecular and cellular mechanisms underlying the cardio-renal-anaemia syndrome and its therapeutics will remain limited.

Since there is a lack of information in the literature concerning animal (rat) models of moderate CKD[7,9-12], we intended to perform a more complete characterization of this model, by assessing hemorheological, biochemical and cardiovascular profiles in a CKD induced by partial (¾) nephrectomy.

MATERIAL AND METHODS

Animals, diets and blood pressure measurement

Male Wistar rats (Charles River Laboratories Inc., Barcelona, Spain), 250-300g, were maintained in an air conditioned room, subjected to 12-h dark/light cycles and given standard laboratory rat chow (IPM-R20, Letica, Barcelona, Spain) and free access to tap water. Animal experiments were conducted according to the European Communities Council Directives on Animal Care.

The rats were divided into 2 groups (7 rats each): a control group and a group with surgical CKD induced by a two-stage (3/4) nephrectomy: firstly, about half of the left kidney was removed by left flank incision and, one week later, the right kidney was removed through a right lateral flank incision. All the animals from the two groups have completed the 15-week study protocol. Body weight (BW) was monitored during the experimental period.

Systolic blood pressure (SBP), diastolic blood pressure (DBP), mean blood pressure (MBP) and heart rate (HR) values were obtained using a tail-cuff sphygmomanometer LE 5001 (Letica, Barcelona, Spain) in appropriate contention cages. Before the measurements, the rats were warmed for 10-20 minutes at 25-30ºC to make the tail artery pulsations detectable and to achieve the pulse level needed. BP and HR values were obtained calculating the average of 8-10 measurements.

Sample collection and preparation

Blood samples: At the beginning of the experiments and at 3, 9 and 15 weeks after the surgical partial nephrectomy the rats were subjected to intraperitoneal anesthesia with a 2 mg/kg BW of a 2:1 (v:v) 50 mg/mL ketamine (Ketalar®, Parke-Davis, Laboratórios Pfeizer, Lda, Seixal, Portugal) solution in 2.5% chlorpromazine (Largactil®, Rhône-Poulenc Rorer, Laboratórios Vitória, Amadora, Portugal). Blood samples were immediately collected by venipuncture from the jugular vein into syringes without anticoagulant (for serum samples collection) or with the appropriate anticoagulant: ethylenediaminetetraacetic acid (EDTA), heparin or a solution of ACD (acid citrate-dextrose). Blood was centrifuged (160 g for 10 min. at 20ºC) to obtain the platelet rich plasma (PRP), which was then centrifuged (730 g for 10 min. at 20ºC) to obtain the platelet pellet and the platelet poor plasma (PPP). In order to maintain a

normal volemia, thus ensuring that results were not changed by the amount of blood collected, some parameters were analyzed only at the final time (15 weeks), namely serum oxidative and inflammatory markers and circulating catecholamines and serotonin contents.

Body and tissues weights and trophism indexes: At the end of experiments, the rats were sacrificed by cervical dislocation and the heart, the adrenals, the kidneys and the liver were immediately removed, placed in ice-cold Krebs' buffer and carefully cleaned of adherent fat and connective tissue. The BW, the whole heart weight (HW), the left ventricle weight (LVW), the adrenals (2: left plus right) weight (AW), and the kidney and liver weights were measured in all the rats under study in order to be used as trophism indexes.

Biochemical assays

Blood lipid: Serum total cholesterol (Total-c), high-density lipoprotein cholesterol (HDL-c), low-density lipoprotein cholesterol (LDL-c) and triglycerides (TGs) were analysed on a Hitachi 717 analyser (Roche Diagnostics Inc., MA, USA) using standard laboratorial methods. The main relationships between the Total-c, HDL-c and LDL-c blood concentrations were calculated to be used as atherogenic and cardiovascular risk indexes (LDL-c/HDL-c and Total-c/HDL-c).

Renal functions and hepatic enzymes: Serum creatinine, ureia and uric acid concentrations were used as renal function indexes and serum aspartate (AST) and alanine amin-

otransferase (ALT) levels were assessed for hepatic evaluation, through automatic validated methods and equipments (Hitachi 717 analyser).

Iron metabolism: Serum iron concentration was determined using a colorimetric method (Iron, Randox Laboratories Ltd., North Ireland, UK), whereas serum ferritin and transferrin were measured by immunoturbidimetry (Laboratories Ltd., North Ireland, UK).

Hematological data

Several hematological parameters were measured in EDTA whole blood by using an automatic Coulter Counter® (Beckman Coulter Inc., USA, CA): red blood cell (RBC) count, haematocrit, haemoglobin (Hb) concentration, hematological indices [mean cell volume (MCV), mean cell Hb (MCH) and mean cell Hb concentration (MCHC)], red cell distribution width (RDW), reticulocyte count, immature reticulocyte fraction (IRF), platelets count, platelets indices [mean platelet volume (MPV), platelet distribution width (PDW) and plaquetocrit (PCT)], and total and differential white blood cells (WBC) counts.

Oxidative equilibrium status

Thiobarbituric acid reactive-species (TBARs) assay: The blood serum was used to determine the products of lipid peroxidation, namely malondialdehyde (MDA), according to a method optimized by Estepa *et al.* (2001)[13].

Ferric reducing antioxidant potential (FRAP) assay: The serum an-

tioxidant capacity was measured as FRAP, according to previously described[14].

Serum 3-nitrotyrosine (3-NT) assay: Serum 3-NT concentration, which is an index of peroxynitrite formation, was quantified by using an enzymatic immunoassay (HyCult biotechnology b.v.; Uden, Netherlands).

Inflammatory markers

Serum levels of interleukin 2 (IL-2), IL-1β, transforming growth factor β1 (TGF-β1) and tumour necrosis factor α (TNF-α) were measured by ultrasensitive Quantikine® ELISA kits (R&D Systems, Minneapolis, USA). Serum C-reactive protein (CRP) was determined by using an ELISA kit from Helica Biosystems, Inc. (Fullerton, CA, USA). All assays were performed in duplicate.

Catecholamine assay

The contents of the catecholamines (CAs) norepinephrine (NE) and epinephrine (E) in the plasma, platelets, adrenals and kidney tissue were evaluated by high performance liquid chromatography with electrochemical detection (HPLC-ED), according to the procedures and chromatographic conditions previously described[15].

NE and E contents were measured by using known concentrations of standards (Sigma Chemical Co., St. Louis, MO, U.S.A.) and the internal standard dihydroxybenzylamine (DHBA), through the peak/area ratio technique. Chromatograms were obtained using the appropriate Gilson 710 software. Concentrations were expressed in: ng/ml for plasma and platelets, μg/g wet tissue for adrenals and ng/g for kidney.

Platelet and plasma serotonergic measures

Platelet and plasma 5-hydroxytryptamine (5-HT) and 5-hydroxindoleacetic acid (5-HIAA) contents were determined by HPLC-ED, according to the preparation/extraction procedures and the chromatographic conditions previously described [15], and calculated using a known concentration of the corresponding standard. Chromatograms were obtained using the appropriate Gilson 710 software. Values were expressed in ng/ml.

Kidney histology

The left kidney tissue of the control rats and the remnant left kidney tissue of the CKD animals were immersion-fixed in 4% buffered paraformaldehyde (PFA) and processed for paraffin sectioning. Three slices from each kidney were embedded. Three micrometre thick sections were stained with the haematoxylin-eosin (H&E). At least 50 glomeruli were evaluated per kidney tissue.

Data Analysis

For statistical analysis, we used the Statview 4.53 software from Abacus Concepts Inc. (Berkeley, CA, USA). Results are presented as means ± standard error of means (s.e.m.).

Comparisons between groups and between different times of evaluation were performed using Factorial ANOVA and Fisher's test. Significance was accepted at *p* less than 0.05.

RESULTS

Biochemical and hematological data

In Tables 1 and 2, we present the biochemical and hemorheological changes for CKD and control rats, before starting experiments and along the experimental period (at 3, 9 and 15 weeks after partial nephrectomy). The results were analysed in order to study the alterations associated with a moderate CKD during 15 weeks of follow-up, as compared to the control group. In CKD rats, three weeks after the partial $(^3/_4)$ nephrectomy, a statistically significant increase in serum urea and creatinine concentrations were found. This increase in renal function markers remained high along the following 12 weeks of the experimental procedure (Table 1).

Concerning to hepatic function markers, a statistically significant increase was found in CKD rats for AST and ALT, particularly for the former at 9 weeks of the experimental period; at the end of experiments (15 weeks) only AST activity was still significantly higher. CKD rats presented alterations in the lipidic profile, namely, a progressively increase in Total-c, TGs and HDL-c (table 1). Iron status evaluation revealed, in CKD rats, a progressively increase in ferritin serum levels, which reached statistical significance in the last evaluation. On the contrary, transferrin serum levels were significantly lower

3 weeks after surgical procedure, and remained lower during the following 12 weeks of follow-up (Table 1).

Concerning to hematological data, 3 weeks after nephrectomy, the CKD animals showed a statistically significant decrease for RBC count, Hb and haematocrit, alongside with a significantly increase in RDW and in platelet count (table 2). These parameters were already similar to those of the control at 9 weeks after surgical intervention and remained stable until the end of the follow-up period. No statistically significant differences were found for total WBC counts; however, neutrophil and eosinophil counts increased progressively in CKD rats. In this group, basophil counts increased 3 weeks after chirurgic procedure, and decreased progressively during the remaining follow-up period, and monocyte counts increased only in the last laboratorial evaluation (Table 2).

Blood pressures, heart rate and body and tissue weights and trophism indexes

At the end of the experimental protocol (15 weeks), a statistically significant increase in SBP, DBP, MBP and HR were found in CKD rats, together with significant increases in heart and left ventricle weights, without any differences in the tissue trophism indexes (Table 3).

Oxidative equilibrium status and inflammatory markers

No statistically significant alterations were found between the two

Table 1. Biochemical changes in a rat model of moderate CKD during a follow-up period of 15 weeks

	Control and CKD rats before partial nephrectomy (n=14)	3 weeks after partial nephrectomy		9 weeks after partial nephrectomy		15 weeks after partial nephrectomy	
		Control (n=7)	CKD (n=7)	Control (n=7)	CKD (n=7)	Control (n=7)	CKD (n=7)
Renal function							
Creatinine (mg/dL)	0.41 ± 0.02	0.40 ± 0.02	0.83 ± 0.04 aa	0.33 ± 0,01	0.81 ± 0.05 aa	0.45 ± 0.02	0.91 ± 0.06 aa
Urea (mg/dL)	41.00 ± 0.68	39.20 ± 0.60	71.00 ± 2.65 a	34.50 ± 1.34	72.80 ± 2.41 aa	39.00 ± 1.58	67.83 ± 2.82 a
Uric acid (mg/dL)	0.60 ± 0.06	0.52 ± 0.05	0.46 ± 0.04	0.34 ± 0.06	0.40 ± 0.04	0.62 ± 0.16	0.48 ± 0.09
Hepatic Enzymes							
AST (IU/L)	68.25 ± 4.73	64.11 ± 3.42	56.70 ± 3.46	51.37 ± 1.21	72.00 ± 3.97 aa	81.00 ± 8.35	141.40 ± 10.83 aaa
ALT (IU/L)	34.00 ± 2.32	32.70 ± 2.31	29.33 ± 1.73	25.32 ± 1.35	39.60 ± 1.63 aaa	33.67 ± 2.32	36.00 ± 2.67
Lipid Profile							
Total-c (mg/dL)	54.33 ± 1,54	51.51 ± 1.49	71.80 ± 4.34 a	43.87 ± 3.12	84.28 ± 6.,51 aaa	55.40 ± 4.01	111.40 ± 5.22 aaa
HDL-c (mg/dL)	44.83 ± 1.22	41.77 ± 1.21	57.87 ± 2.89 a	34.37 ± 2.69	67.57 ± 4.42 aaa	42.60 ± 2.64	81.00 ± 4.18 aaa
LDL-c (mg/dL)	21.02 ± 0.78	19.31 ± 1.22	12.72 ± 1.10 aa	17.49 ± 1.00	15.81 ± 1.57	16.88 ± 1.09	16.01 ± 0.72
TGs (mg/dL)	131.66 ± 4.98	126.71 ± 8.82	84.20 ± 7.84	111.00 ± 10.28	162.40 ± 35.64	139.00 ± 21.24	207.00 ± 38.25 a
LDL-c/HDL-c	0.47 ± 0.03	0.48 ± 0.04	0.22 ± 0.02 aa	0.53 ± 0.04	0.25 ± 0.05 aaa	0.40 ± 0.05	0.20 ± 0.02 a
Total-c/HDL-c	1.21 ± 0.02	1.24 ± 0.02	1.21 ± 0.02	1.29 ± 0.04	1.24 ± 0.02	1.30 ± 0.04	1.38 ± 0.05
Iron metabolism							
Iron (μg/dL)	153.16 ± 12.89	108.91 ± 16.52	145.25 ± 8.74	194.27 ± 5.70	155.28 ± 7.51	154.20 ± 26.92	124.50 ± 11.91
Ferritin (ng/mL)	12.63 ± 1.35	12.02 ± 1.39	17.96 ± 1.12	10.01 ± 1.05	21.32 ± 2.14	12.92 ± 3.68	24.66 ± 5.32 a
Transferrin (mg/dL)	130.33 ± 3.79	130.91 ± 3.64	104.80 ± 2.79 aa	130.00 ± 2.47	106.01 ± 5.79aa	120.00 ± 7.97	81.57 ± 11.02 aaa

AST: aspartate aminotransferase; ALT: alanine aminotransferase; CKD: chronic kidney disease; HDL-c: high density lipoprotein-cholesterol; LDL-c: low density lipoprotein-cholesterol; TGs: triglycerides; Total-c: serum total cholesterol. Results are presented as mean ± s.e.m.: a – $p < 0.05$, aa – $p < 0.01$ and aaa – $p < 0.001$ vs the control group

Table 2. Hematological changes in a rat model of moderate CKD during a follow-up period of 15 weeks

	Control and CKD rats before partial nephrectomy (n=14)	3 weeks after partial nephrectomy		9 weeks after partial nephrectomy		15 weeks after partial nephrectomy	
		Control (n=7)	CKD (n=7)	Control (n=7)	CKD (n=7)	Control (n=7)	CKD (n=7)
RBC parameters							
Hb (g/dL)	13.82 ± 0.14	13.52 ± 0.21	11.42 ± 0.22 a	12.90 ± 0.18	13.70 ± 0.22	13.94 ± 0.36	13.44 ± 0.20
Haematocrit (%)	39.50 ± 0.49	38.61 ± 0.50	32.81 ± 0.62 a	36.34 ± 0.52	40.20 ± 0.21	40.92 ± 0.71	39.54 ± 0.57
RBC (x1012/L)	7.32 ± 0.12	7.13 ± 0.11	6.18 ± 0.12 a	6.39 ± 0.08	7.25 ± 0.19	7.44 ± 0.10	6.91 ± 0.14
MCV (fL)	53.95 ± 0.62	54.71 ± 0.53	53.09 ± 0.48	57.04 ± 0.64	55.54 ± 0.72	55.04 ± 1.32	57.27 ± 0.66
MCH (pg)	18.85 ± 0.25	19.23 ± 0.23	18.49 ± 0.17	20.20 ± 0.25	18.96 ± 0.36	18.74 ± 0.61	19.48 ± 0.28
MCHC (g/dL)	34.93 ± 0.19	34.91 ± 0.20	34.84 ± 0.13	35.43 ± 0.15	34.14 ± 0.33	34.04 ± 0.37	34.00 ± 0.30
RDW (%)	13.33 ± 0.43	13.23 ± 0.31	15.27 ± 0.35 a	12.58 ± 0.36	13.00 ± 0.20	14.88 ± 0.39	13.54 ± 0.23
Reticulocytes (x109/L)	389.01 ± 29.10	393.11 ± 22.97	423.09 ± 20.01	379.11 ± 39.95	392.09 ± 34.04	383.98 ± 28.97	326.09 ± 27.02
IRF (%)	0.38 ± 0.02	0.39 ± 0.03	0.41 ± 0.02	0.52 ± 0.07	0.42 ± 0.05	0.38 ± 0.01	0.56 ± 0.09
WBC parameters							
WBC (x109/L)	6.87 ± 1.19	6.51 ± 1.02	6.69 ± 0.38	5.14 ± 0.91	6.39 ± 0.29	5.14 ± 0.22	5.53 ± 0.85
Neutrophils (x109/L)	0.08 ± 0.01	0.07 ± 0.01	0.10 ± 0.01	0.05 ± 0.01	0.25 ± 0.17 a	0.07 ± 0.01	0.52 ± 0.31 a
Lymphocytes (x109/L)	5.82 ± 1.04	5.51 ± 0.81	4.38 ± 0.43	4.37 ± 0.79	4.86 ± 0.34	4.32 ± 0.81	4.65 ± 0.74
Basophils (x109/L)	1.15 ± 0.33	1.01 ± 0.22	1.89 ± 0.30 a	0.65 ± 0.15	1.25 ± 0.23 a	0.91 ± 0.52	0.29 ± 0.18 a
Eosinophils(x109/L)	0.012 ± 0.002	0.015 ± 0.003	0.023 ± 0.003	0.015 ± 0.003	0.028 ± 0.004 a	0.023 ± 0.007	0.064 ± 0.032 a
Monocytes (x109/L)	0.007 ± 0.002	0.006 ± 0.002	0.009 ± 0.003	0.005 ± 0.002	0.001 ± 0.001	0.004 ± 0.002	0.018 ± 0.010 a
Platelet parameters							
Platelets (x109/L)	980.50 ± 22.79	973.41 ± 22.62	1203.80 ± 47.93 a	943.87 ± 32.60	938.43 ± 49.85	980.40 ± 33.07	943.85 ± 78.49
PCT (%)	0.57 ± 0.02	0.56 ± 0.02	0.66 ± 0.02 a	0.54 ± 0.02	0.51 ± 0.02	0.58 ± 0.02	0.56 ± 0.03
MPV (fL)	5.83 ± 0.17	5.73 ± 0.12	5.53 ± 0.07	5.69 ± 0.07	5.50 ± 0.08	5.90 ± 0.14	5.70 ± 0.11
PDW (%)	16.15 ± 0.21	16.22 ± 0.19	15.99 ± 0.14	16.30 ± 0.24	16.04 ± 0.23	16.68 ± 0.26	16.60 ± 0.22

CKD: chronic kidney disease; Hb: hemoglobin; IRF: immature reticulocyte fraction; MCH: mean corpuscular hemoglobin; MCHC: mean corpuscular hemoglobin concentration; MCV: mean corpuscular volume; MPV=Mean platelet volume; PCT: plateletocrit; PDW: platelet distribution width; RBC: red blood cell; RDW: red deviation weight; WBC: white blood cell. Results are presented as mean ± s.e.m.: a – $p < 0.05$, aa – $p < 0.01$ and aaa – $p < 0.001$ vs the control group

Table 3. Blood pressures, heart rate and body and tissue weights and trophism indexes in a rat model of moderate CKD after an experimental period of 15 weeks

	Control (n=7)	CKD (n=7)
Blood Pressures and Heart Rate		
SBP (mmHg)	114.88 ± 3.08	143.07 ± 4.61 aaa
DBP (mmHg)	99.11 ± 1.76	123.31 ± 12.38 aa
MBP (mmHg)	104.33 ± 1.89	129.64 ± 9.79 aaa
HR (beats/min.)	339.12 ± 6.28	391.89 ± 12.00 aaa
Body and Tissue Weights		
BW (Kg)	0.47 ± 0.02	0.46 ± 0.01
HW (g)	1.21 ± 0.03	1.46 ± 0.06 a
LVW (g)	0 .57 ± 0.03	0.72 ± 0.04 a
KW (g)	1.24 ± 0.04	1.94 ± 0.20
LW (g)	15.91 ± 0.58	18.23 ± 0.77
AW (g)	0.09 ± 0.01	0.10 ± 0.01
Tissue Trophism Indexes		
HW/BW (g/kg)	2.65 ± 0.07	2.98 ± 0.10
LVW/HW (g/kg)	0.47 ± 0.02	0.50 ± 0.02
LVW/BW (g/kg)	1.05 ± 0.11	1.17 ± 0.14
KW/BW (g/kg)	2.62 ± 0.05	3.96 ± 0.39
LW/BW (g/kg)	33.90 ± 0.10	38.80 ± 2.51
AW/BW (g/kg)	0.18 ± 0.02	0.20 ± 0.02

AW: adrenals weight; BW: body weight; CKD: chronic kidney disease; DBP: diastolic blood pressure; HR: heart rate; HW: heart weight; KW: kidney weight; LVW: left ventricle weight; LW: liver weight; MBP: mean blood pressure; SBP: systolic blood pressure. Results are presented as mean ± s.e.m.: a – $p < 0.05$, aa – $p < 0.01$ and aaa – $p < 0.001$ *vs* the control group

rats groups for MDA and TAS, but a significantly higher serum concentration of 3-NT was found. Concerning the inflammatory profile, we observed no significant differences between the two groups for CRP, IL-1β, IL-2 and TNF-α, excepting for TGF-β1 that augmented in CKD rats (Table 4).

Catecholamine and serotonin measures

Concerning sympathetic activity, CKD rats presented a statistically significant increase in plasma and kidney NE, and a decrease in platelet content;

a significant reduction in platelet and adrenals E, and a concomitant increment in plasma E concentration were also observed (Fig. 1). Peripheral serotonergic measures in the CKD rats after the 15 weeks of follow-up showed a trend to higher values for all parameters, when compared to control animals, even though a statistically significant augment was only found for platelet 5-HIAA (Fig. 2).

Kidney morphology

The kidney morphology of the CKD rats was distinct from that of the controls (Fig. 3). The glomerular

Table 4. Redox state and inflammatory markers in a rat model of moderate CKD after an experimental period of 15 weeks

	Control (n=7)	CKD (n=7)
Redox State		
MDA (μmol/L)	0.27 ± 0.05	0.34 ± 0.06
TAS (μmol/L)	394.72 ± 51.42	408.03 ± 23.62
MDA/TAS	0.56 ± 0.05	0.73 ± 0.21
3-NT (nmol/L)	15.66 ± 1.40	50.45 ± 3.22 aaa
Inflammatory Profile		
CRP (μg/mL)	24.78 ± 1.25	25.83 ± 0.66
IL-1β (pg/mL)	26.52 ± 0.94	23.76 ± 0.99
IL-2 (pg/mL)	36.28 ± 8.70	49.34 ± 3.43
TGF-β1 (pg/mL)	358.41 ± 34.52	544.42 ± 50.43 a
TNF-α (pg/mL)	16.34 ± 1.81	15.75 ± 1.96

CKD: chronic kidney disease; CRP: C-reactive protein; IL-1β: interleukin 1β; IL-2: interleukin 2; MDA: malondialdehyde; TAS: total antioxidant status; TGF-β1: transforming growth factor β1; TNF-α: tumour necrosis factor α; 3-NT: 3-nitrotyrosine. Results are presented as mean ± s.e.m.: a – $p < 0.05$, aa – $p < 0.01$ and aaa – $p < 0.001$ *vs* the control group

capillary tufts of the CKD rats were hypercellular, with an increment of the glomerular volume. The Bowman space was also higher (Fig. 3B1). The interstitial region was lower due to tubular atrophy, together with an expansion of proximal convoluted tubules (Fig. 3B2).

DISCUSSION

Early detection of CKD and initiation of treatment should contribute to prevent or delay some of these adverse effects[16]. However, animal models of moderate CKD, which might be good tools to study the pathophysiological mechanisms underlying intermediary stages of renal disease and the efficacy of therapeutics, remain to be fully characterized. Our results have confirmed that the surgical partial (3/4) nephrectromy produces a moderate, but sustained stage of CKD. Indeed, we observed a significant (but restrained) increase in serum urea and creatinine concentrations at 3 weeks after the surgery that remained almost constant during the following period (still significantly higher than controls).

Furthermore, the results observed for RBC and reticulocyte counts, were similar to those observed for serum urea and creatinine along the follow-up period, further strengthens that a moderate stage of CKD was generated. RBC count was significantly lower 3 weeks after nephrectomy, consistent with the development of anaemia secondary to renal mass reduction; moreover, the number of reticulocytes, as well as the percentage of immature reticulocytes did not increase, further supporting a failure of the erythropoietic response mechanisms, due to insufficient erythropoietin production associated to the reduction in renal tissue. However, the anaemia was notoriously transitory, as both RBC and reticulo-
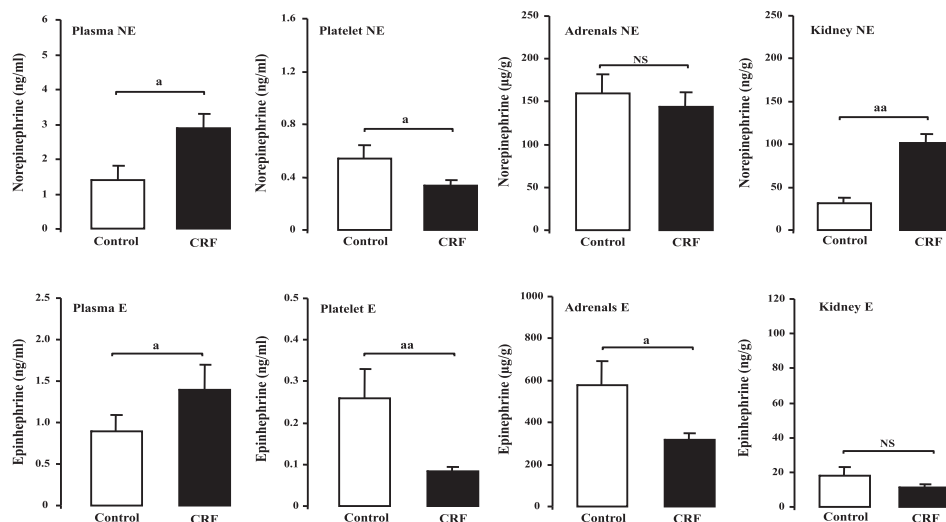
Patrícia Garrido et al.
FIGURE 1

Fig. 1. Norepinephrine and epinephrine contents in plasma, platelets, adrenals and kidneys in a rat model of moderate CKD after an experimental period of 15 weeks. E: epinephrine; NE: norepinephrine. Results are presented as mean ± s.e.m.: a – $p<0.05$, aa – $p<0.01$ and aaa – $p<0.001$ vs the control group. NS: non-significant

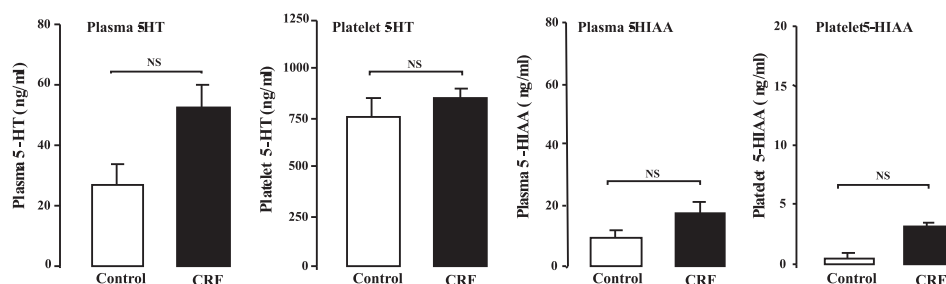*Patrícia Garrido et al.*
FIGURE 2

Fig. 2. Plasma and platelet 5-HT and 5-HIAA in a rat model of moderate CKD after an experimental period of 15 weeks. 5-HT: 5-hydroxy-tryptamine; 5-HIAA: 5-hydroxyindoleacetic acid. Results are presented as mean ± s.e.m.: NS: non-significant

cyte values returned to normal values in the following evaluation points (9 and 15 weeks of study), suggesting that our model is a moderate (but yet functional) CKD. This pattern is also confirmed by the low-grade histomorphological changes (lesions) found in the kidneys of CKD rats. There was also a trend to increased kidney weight (hypertrophy), consistent with a compensated renal insufficiency. Similar hypertrophy was obtained in other models of chronic renal failure induction, such as the 5/6 nephrectomized rats[9-12].

Iron-restricted erythropoiesis is a common clinical condition in patients with CKD. Several causes were proposed to underlie this situation, such as a functional iron deficiency, inadequate dietary iron intake, blood loss during the haemodialysis processes or from gastrointestinal tract (bleeding), inadequate intestinal iron ab-
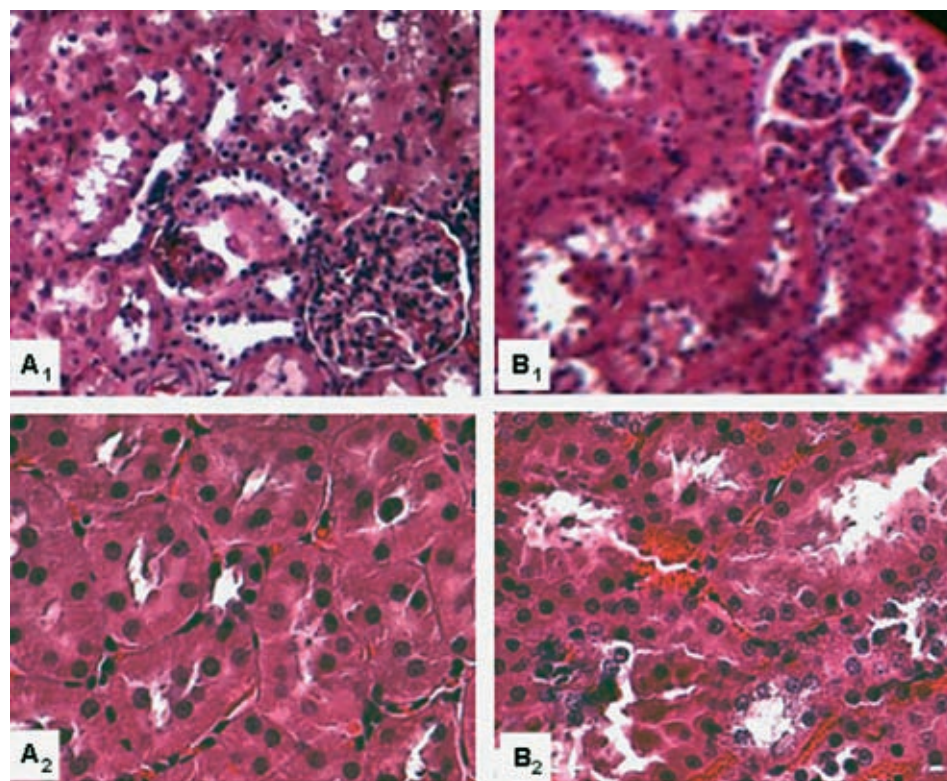
Fig. 3. Renal histology of kidneys from control (A) and moderate chronic CKD rats (B): 1 – glomerular region; 2 – proximal convoluted tubules area (original amplification x10 and x40, respectively for figures 1 and 2).

sorption and inhibition of iron mobilization from macrophages[17]. In our study, CKD rats presented serum iron values similar to those of the control and no significant changes were observed along the experiments; however, a trend towards higher values of ferritin were observed along the experiments and reached a significantly higher value at the end (15 weeks); these changes in ferritn were accompanied by a significant reduction in transferrin (observed at 3 weeks and afterwards), suggesting an inhibition in iron traffic, from macrophages to erythroid cells, leading to the progressive increase in iron storage, as showed by the progressive increase in ferritin, observed throughout the experiments. This suggests that our moderate model of CKD could also be used as a model of functional iron deficiency. Indeed, a functional iron deficiency has been reported in CKD patient under hemodialysis, namely, in moderate stages[17,18].

Liver metabolism dysfunction should plays a role in the lipid profile changes encountered in the CKD rats: increased values of total-cholesterol, HDL-c and TGs, without differences on LDL-c content, which might be explained, at least in part, by the lack in cholesteryl ester transfer protein (CETP), a characteristic of the rats[19,20]. Lipid abnormalities are found in CKD humans and the prevalence of hyperlipidaemia is higher than in the general population[21,22]. However, the risk of cardiovascular disease in CKD patients varies depending on the type of lipid abnormalities, the cause of renal disease and the degree of reduction in

glomerular filtration rate (GFR)[23]. Our rat model reproduces the changes encountered in CKD patients, in whom the main features are an increased serum level of both VLDL and IDL fractions, leading to hypertriglyceridemia and an unchanged or slightly increased LDL fraction enriched with triacylglycerols that might be attributed to the slow catabolism of the triacylglycerol-rich lipoproteins[24-26].

Besides the anaemia secondary to CKD, patients usually develop cardiac failure that further aggravates renal disease [2, 27, 28]. This triad of dysfunctions, already known as cardio-renal anaemia syndrome, is responsible for the serious complications encountered in those patients. Our study intended to clarify the degree of cardio-renal complications associated with this model of moderate CKD. Hypertension is a well established cause, a common complication, and an important risk factor for progression of the cardiovascular complications and the mortality of patients with CKD[4,5]; the pathophysiology of this hypertension is multifactorial[4]. Several authors conclude that CKD also activates (through the renin-angiotensin system participation) the sympathetic nervous system (SNS)[1]. Our results obtained using an animal model seem to be in agreement with the data from humans with CKD, despite a direct extrapolation from rat studies to humans deserves careful interpretation. In any case, an increased systolic and diastolic blood pressure was obtained, together with tachycardia and heart and left ventricle hypertrophy, which should be due to additional heart (left ventricle) effort to compensate the renal func-

tion deterioration. The kidneys, strategically positioned, have dense sensory and efferent sympathetic innervations, and can be the origin, as well as the target of overactivity of the SNS, which has been convincingly shown in CKD animal models[29]. Several studies showed that sub-totally nephrectomized rats developed a rapid increase of BP within a week after renal ablation, while totally nephrectomized rats, in which afferent sensory signals were removed, did not develop hypertension. This suggests that afferent signals from the disease kidneys are transmitted to the vasomotor control centre in the brain, thereby contributing to the increased blood pressure[1]. In our model of moderate CKD, plasma norepinephrine and epinephrine contents were increased, which might be caused by adrenal and platelet release, due to sympathetic system overactivation and platelet hyperreactivity, respectively. Moreover, plasma 5-HT was also increased, which, together with catecholamine increment, might influence platelet and vascular reactivity and, thus, contributing to cardiovascular and thromboembolic complications, as found in CKD patients[30-32].

Other factors have been studied to clarify the causes of the hypertension observed in CKD patients, including high levels of endothelin, oxidative stress or nitric oxide (NO) reduction[4,33-35]. In CKD patients, oxidative stress and inflammation could play a crucial role in the pathogenesis of the atherosclerosis, malnutrition and anaemia. In our model of moderate CKD, the redox state seems to be unaltered (MDA/TAS ratio was unchanged) which might be due to a

proper compensation of ROS formation by antioxidants. However, there was an increased serum 3-NT value, which is a marker of peroxynitrite generation, and, thus, might hypothetically reflect an increased superoxide formation and, thus, a reduced NO availability, since this dangerous oxidant is formed by the combination of both. In this model, inflammation seem to be yet less relevant, since, excepting an increment of TGF-β1, all the other markers were unchanged. The increment in ferritin, an acute phase protein, might also be viewed as part of an inflammatory state. The involvement of inflammation on this model of moderate CKD should be further confirmed, namely, by studies on the hypertrophic remnant kidney.

In conclusion, our model is consistent with a moderate but sustained degree of CKD with a compensated anaemia, though presenting a disturbance in iron metabolism. Despite the reasonable degree of functionality of the remnant kidney, as suggested by the correction of anaemia as well as by the kidney hypertrophy, several important cardiovascular modifications were developed. Therefore, our model presented hypertension, dyslipidaemia, sympathetic activation and oxidative stress. This model might be a good tool to study the cellular and molecular pathophysiological mechanisms underlying moderate stages of CKD, as occurs in humans, and, even more relevant, to evaluate the efficacy of therapeutics for prevention, treatment or correction of cardio-renal anaemia syndromes and complications in early stages.

REFERENCES

1. Rump LC, Amann K, Orth S, *et al.* Sympathetic overactivity in renal disease: a window to understand progression and cardiovascular complications of uraemia? Nephrol Dial Transplant 2000; 15:1735-1738.
2. Parmar MS. Chronic Renal Disease. BMJ 2002; 325:85-90.
3. Stenvinkel P. Anaemia and inflammation: what are the implications for the nephrologists? Nephrol Dial Transplant 2003; 18:viii17-viii22.
4. Koomans HA, Blankestijn PJ, Joles JA. Sympathetic hyperactivity in chronic renal failure: a wake-up call. J Am Soc Nephrol 2004; 15:524-537.
5. Costa E, Pereira BJ, Rocha-Pereira P, *et al.* Role of prohepcidin, inflammatory markers and iron status in resistance to rhEPO therapy in hemodialysis patients. Am J Nephrol 2008;28:677-683.
6. Bakris GL. Protecting renal function in the hypertensive patient: clinical guidelines. Am J Hypertens 2005; 18:112S-119S.
7. Liu ZC, Chow KM, Chang TM. Evaluation of two protocols of uremic rat model: partial nephrectomy and infarction. Ren Fail 2003; 25:935-943.
8. Ofstad J, Horvei G, Kvam FI, *et al.* Glomerular hemodynamics in progressive renal disease. Kidney Int 1992; 36:S8-S14.
9. Fine L. The biology of renal hypertrophy. Kidney Int 1986; 29:619-634.
10. Gretz N, Waldherr R, Strauch M. The remnant kidney model; in Gretz N, Strauch M (Eds.). Experimental and genetic rat models of chronic renal failure. Basel, Karger, 1993; 1-28.
11. Hostetter TH, Olson JL, Rennke HG, *et al.* Hyperfiltration in remnants nephrons: a potentially adverse response to renal ablation. J Am Soc Neprol 2001; 12:1315-1325.
12. Perez-Ruiz L, Ros-Lopez S, Cardús A, *et al.* A forASTten method to induce experimental chronic renal failure in the rat by ligation of the renal parenchyma. Nephron Exp Nephrol 2006; 103(3):e126-e130.
13. Estepa V, Ródenas S, Martín MC: Optimización de un método para la determinación de la peroxidación lipídica en suero humano. Anal Real Acad Farm 2001; 67:1-17.
14. Benzie IFF, Strain JJ. The Ferric Reducing Ability of Plasma (FRAP) as a Measure of ''Antioxidant Power'': The FRAP Assay. Anal Biochem 1996; 239:70-76.
15. Reis F, Rocha L, Ponte L, *et al.* Effect of preventive and regressive isosorbide 5-mononitrate treatment on catecholamine levels in plasma, platelets, adrenals, left ventricle and aorta in cyclosporin A-induced hypertensive rats. Life Sci 2005; 77:2514-2528.
16. Remuzzi G, Ruggenenti P, Perico N. Chronic renal diseases: renoprotective benefits of renin-angiotensin system inhibition. Ann Intern Med 2002; 136:604-615.
17. Hörl WH. Iron therapy for renal anemia: how much needed, how much harmful? Pediatr Nephrol 2007; 22:480-489.
18. Brugnara C. Iron deficiency and erythropoiesis: new diagnostic approaches. Clin Chem 2003; 49:1573-1578.

19. Oschry Y, Eisenberg S. Rat plasma lipoproteins: reevaluation of a lipoprotein system in an animal devoid of cholesteryl ester transfer activity. J Lipid Res 1982; 23:1099-1106.

20. Vaziri ND, Liang K. ACAT inhibition reverses LCAT deficiency and improves plasma HDL in chronic renal failure. Am J Physiol Renal Physiol 2004; 287:F1038-F1043.

21. Kasiske BL. Hyperlipidemia in patients with chronic renal disease. Am J Kidney Dis 1998; 32:S142-153.

22. Tsimihodimos V, Dounousi E, Siamopoulos KC. Dyslipidemia in chronic kidney disease: an approach to pathogenesis and treatment. Am J Nephrol 2008; 28:958-73.

23. Chan CM. Hyperlipidemia in chronic renal disease. Ann Acad Med Singapore 2005; 35:31-35.

24. Grundy SM: Management of hyperlipidemia of kidney disease. Kidney Int 1990; 37:847-853.

25. Attman PO, Samuelsson O, Alaupovic P. Lipoprotein metabolism and renal failure. Am J Kidney Dis 1993; 21:573-592.

26. Szolkiewicz M, Nieweglowski T, Korczynska J, *et al.* Upregulation of fatty acid synthase gene expression in experimental chronic renal failure. Metabolism 2002; 51:1605-10.

27. Silverberg D, Wexler D, Blum M, *et al.* The cardio-renal anaemia syndrome: does it exist? Nephrol Dial Transplant 2003; 18:viii7-viii12.

28. Wexler D, Silverberg D, Blum M, *et al.* Anaemia as a contributer to morbidity and mortality in congestive heart failure. Nephrol Dial Transplant 2005; 20:vii11-vii15.

29. Campese VM. Neurogenic factors and hypertension in chronic renal failure. J Nephrol 1997; 10:184-187.

30. Vanhoutte PM. Platelet-derived serotonin, the endothelium, and cardiovascular disease. J Cardiovasc Pharmacol 1991; 17:S6-12.

31. Azzadin A, Mysliwiec J, Wollny T, *et al.* Serotonin is involved in the pathogenesis of hypertension developing during erythropoietin treatment in uremic rats. Thromb Res 1995; 77:217-224.

32. Malyszko J, Malyszko JS, Pawlak D, *et al.* Homeostasis, platelet function and serotonin in acute and chronic renal failure. Thromb Res 1996; 83:351-361.

33. Ritz E, Koomans HA. New insights into mechanisms of blood pressure regulation in patients with uraemia. Nephrol Dial Transplant 1996; 11:52–59.

34. Pechter U, Aunapuu M, Riispere Z, *et al.* Oxidative stress status in kidney tissue after losartan and atenolol treatment in experimental renal failure. Nephron Exp Nephrol 2004; 97:e33-7.

35. Manning RD Jr, Tian N, Meng S. Oxidative stress and antioxidant treatment in hypertension and the associated renal damage. Am J Nephrol 2005; 25:311-317.

RED BLOOD CELL STORAGE DURATION AND MORTALITY IN PATIENTS UNDERGOING PERCUTANEOUS CORONARY INTERVENTION

Robinson SD[1], Janssen C[1], Fretz EB[1], Berry B[1], Chase AJ[1], Siega AD[1], Carere RG[1], Fung A[1], Simkus G[1], Klinke WP[1], Hilton JD[1]

BACKGROUND: Blood transfusion has been associated with an increased mortality in patients undergoing percutaneous coronary intervention (PCI). Although the reasons for this remain unclear, it may be related to the structural and functional changes occurring within red blood cells (RBCs) during storage. We investigated whether RBC storage duration was associated with mortality in patients requiring transfusion after PCI. METHODS: We collected data on all RBC transfusions occurring within 10 days of PCI (excluding those related to cardiac surgery) using the British Columbia Cardiac Registry and Central Transfusion Registry. Transfusion details were analyzed according to 30-day survival. RESULTS: From a total of 32,580 patients undergoing PCI, 909 (2.8%) patients received RBCs with a mean storage duration of 25 +/- 10 days. In these 909 patients, mean transfusion volumes were lower in survivors (2.8 +/- 2.1 vs 3.8 +/- 2.9 U, P = .002) than those who died within 30 days. In a multivariate analysis to adjust for baseline risk, mean RBC storage age (HR 1.02 [95% CI 1.01-1.04], P = .002) and transfusion volume (HR 1.26 [95% CI 1.18-1.34], P < .001) both predicted 30-day mortality. Transfused patients who received only older blood (RBC min age >28 days) appeared to be at greater risk of death (HR 2.49 [95% CI 1.45-4.25], P = .001). CONCLUSION: Red blood cell transfusion is associated with increased 30-day mortality in patients undergoing PCI. Although current transfusion practice permits RBC storage for up to 42 days, the use of older red cells may pose an additional hazard to this patient group. 2010 Mosby, Inc. All rights reserved **[Am Heart J. 2010; 159(5):876-81]**

PMID: 20435199

[1] Victoria Heart Institute Foundation, Victoria BC, Canada
 e-mail: sdrobinson@vhif.org

NATURAL HISTORY OF EXPERIMENTAL CORONARY ATHEROSCLEROSIS AND VASCULAR REMODELING IN RELATION TO ENDOTHELIAL SHEAR STRESS. A SERIAL, IN VIVO INTRAVASCULAR ULTRASOUND STUDY.

Koskinas KC[1], Feldman CL[1], Chatzizisis YS[1], Coskun AU[1], Jonas M[1], Maynard C[1], Baker AB[1], Papafaklis MI[1], Edelman ER[1], Stone PH[1]

BACKGROUND: -The natural history of heterogeneous atherosclerotic plaques and the role of local hemodynamic factors throughout their development are unknown. We performed a serial study to assess the role of endothelial shear stress (ESS) and vascular remodeling in the natural history of coronary atherosclerosis. Methods and Results-Intravascular ultrasound-based 3-dimensional reconstruction of all major coronary arteries (n=15) was performed serially *in vivo* in 5 swine 4, 11, 16, 23, and 36 weeks after induction of diabetes mellitus and hyperlipidemia. The reconstructed arteries were divided into 3-mm-long segments (n=304). ESS was calculated in all segments at all time points through the use of computational fluid dynamics. Vascular remodeling was assessed at each time point in all segments containing significant plaque, defined as maximal intima-media thickness >/=0.5 mm, at week 36 (n=220). Plaque started to develop at week 11 and progressively advanced toward heterogeneous, multifocal lesions at all subsequent time points. Low ESS promoted the initiation and subsequent progression of plaques. The local remodeling response changed substantially over time and determined future plaque evolution. Excessive expansive remodeling developed in regions of very low ESS, further exacerbated the low ESS, and was associated with the most marked plaque progression. The combined assessment of ESS, remodeling, and plaque severity enabled the early identification of plaques that evolved to high-risk lesions at week 36. Conclusions-The synergistic effect of local ESS and the remodeling response to plaque formation determine the natural history of individual lesions. Combined *in vivo* assessment of ESS and remodeling may predict the focal formation of high-risk coronary plaque. **[Circulation, 2010;121 (19):2092-101]**

PMID: 20439786

[1] Cardiovascular Division, Brigham and Women's Hospital, Harvard Medical School, Boston, Massachusetts

EVALUATION OF SUBLINGUAL AND GUT MUCOSAL MICROCIRCULATION IN SEPSIS: A QUANTITATIVE ANALYSIS

Verdant CL[1], De Backer D[1], Bruhn A[1], Clausi CM[1], Su F[1], Wang Z[1], Rodriguez H[1], Pries AR[1], Vincent JL[1].

OBJECTIVE: To determine the relationship between sublingual and intestinal mucosal microcirculatory perfusion. DESIGN: Observational, experimental study. SETTING: University-affiliated large animal laboratory. SUBJECTS: Ten fasted, anesthetized, mechanically ventilated, male pigs randomized to a sham group (n = 3) or to a hyperdynamic septic shock group (n = 7) in which cholangitis was induced by direct infusion of Escherichia coli into the common bile duct. This model was developed because it is not accompanied by changes in intra-abdominal pressure. MEASUREMENTS AND MAIN RESULTS: The sublingual and intestinal microcirculations were simultaneously assessed at 4-hr intervals for up to 12 hrs with a modified orthogonal polarization spectral device and functional microvessel density and erythrocyte velocity were measured quantitatively. In sham animals, both regions maintained a stable functional microvessel density and erythrocyte velocity throughout the study period. In contrast, in septic animals, already after 4 hrs of sepsis, functional microvessel density was markedly decreased (>50%) in the sublingual and gut regions; mean erythrocyte velocity decreased dramatically and similarly in both regions, from 1022 +/- 80 to 265 +/- 43 mum/sec in the sublingual region and from 1068 +/- 45 to 243 +/- 115 mum/sec in the gut (p < 0.001, at T12). There was a significant correlation between the sublingual and gut microcirculations in septic animals (r = 0.92, p < 0.0001). CONCLUSIONS: The severity and the time course of microcirculatory changes were similar in the sublingual and in the gut region in this clinically relevant model of severe sepsis. These findings support the sublingual region as an appropriate region to monitor the microcirculation in sepsis. **[Crit Care Med. 2009; 37(11):2875-81]**

[1] Department of Intensive Care, Erasme Hospital, Université libre de Bruxelles, Brussels, Belgium
e-mail: jlvincen@ulb.ac.be

REUNIÃO CIENTÍFICA

16.ª CONFERÊNCIA DA SOCIEDADE EUROPEIA DE HEMORREOLOGIA CLÍNICA E MICROCIRCULAÇÃO

Munique (Alemanha), 2011, será o palco da 16.ª Conferência Europeia de Hemorreologia Clínica e Microcirculação (ESCHM), sob a presidência do Prof. D. Clevert. O evento decorrerá em conjunto, pela primeira vez, em conjunto com a Sociedade Internacional de Hemorreologia Clínica e Micro-circulação (ISCH) e Sociedade Internacional de Biorreologia (ISB).

Para mais informações consultar o sítio da ESCHM:

http://www.unisi.it/ricerca/asso/esch/index.htm

REGRAS DE PUBLICAÇÃO / INSTRUCTIONS TO AUTHORS

CONVITE

A Sociedade Portuguesa de Hemorreologia e Microcirculação (SPHM) aceita para publicação no seu BOLETIM artigos de curta extensão. O Boletim é editado quatro vezes por ano em formato de papel e electrónico (www.hemorreologia.com), sendo), sendo distribuído gratuitamente aos sócios, individualidades e instituições científicas e culturais.

INSTRUÇÕES

1. Todos os textos enviados para publicação estão sujeitos a apreciação editorial e aprovação. A decisão é baseada no mérito científico e cultural dos trabalhos.

2. São aceites somente os trabalhos preparados em versão óptica (*PDF* ou *Microsoft Word*).

3. Os textos devem ser redigidos em Português ou Inglês.

4. Os manuscritos com o pedido de publicação devem ser enviados por *e-mail* ao Editor (carlotasaldanha@fm.ul.pt).

– Comunicações Originais (artigos curtos) – Os textos serão considerado para publicação rápida, com a seguinte estrutura: Sumário (50-70 palavras), Introdução, Material e Métodos, Resultados, Discussão e Conclusões. O(s) autor(es) são estimulados a englobar em conjunto os resultados, discussão e conclusões.
(Extensão máxima do texto: 5 a 6 páginas a um espaço (letra de corpo 11), incluindo figuras tabelas e quadros(e respectivas legendas),agradecimentos e até 30 referências bibliográficas).

– Artigos de Revisão – O BOLETIM terá a maior satisfação em acolher curtas revisões sobre assuntos de particular interesse, no âmbito da Hemorreologia, Microcirculação ou assuntos de âmbito médico ou de outras áreas científicas afins, que sejam submetidos directamente para publicação ou mediante convite especial do Editor.
(Extensão máxima do texto:8 a 10 páginas (letra de corpo 11) incluindo figuras, tabelas, quadros, fotos (e respectivas legendas), agradecimentos e até 60 referências bibliográficas).

INVITATION

The Portuguese Society on Hemorheology and Microcirculation (Sociedade Portuguesa de Hemorreologia e Microcirculação, SPHM) is pleased to welcome short papers for publication in its BOLETIM. This publication, in paper and online (www.hemorreologia.com), is distributed four times a year free of charge to the members of the Society.

INSTRUCTIONS

1. All submitted manuscripts are subjected to editorial review and approval. The decision to publish is dependent on the scientific and cultural merit of the papers.

2. Only contributions prepared and submitted as optic version (*PDF* or *Microsoft Word*), will be accepted.

3. Texts must be written in Portuguese or in English.

4. All scientific contributions, including manuscript submission and further correspondence should be addressed by *email* to the Editor (carlotasaldanha@fm.ul.pt)

– Original Communications – Manuscripts may be considered for rapid processing as short communications. All manuscripts should be arranged in the following sections: Abstract (50-70 words), Introduction, Material and Methods, Results, Discussion, Acknowledgements and References. The author(s) may combine some of the sections normally included in a full paper, namely the results, discussion and conclusions.
(Maximum communication length – 5-6 single spaced typed pages, including figures, tables, legends, acknowledgments and up to 30 references).

– Short Reviews – The BOLETIM will publish reviews on subjects of particular interest in its field, either following a special invitation or a submission by the author, and in the latter case only after approval by an Editorial Board member. Further information can be obtained from the editor.
(Maximum review length – 8-10 full pages, including figures, tables, photos, legends, acknowledgments and up to 60 references)